IOP Publishing Journal of Physics: Condensed Matter
J. Phys.: Condens. Matter **32** (2020) 195503 (8pp) https://doi.org/10.1088/1361-648X/ab6ae8

Undulated silicene and germanene freestanding layers: why not?

M-C Hanf[1,2,4], A Marjaoui[1,2,3], R Stephan[1,2], M Zanouni[3], M Diani[3] and Ph Sonnet[1,2]

[1] Université de Haute Alsace, CNRS, IS2M UMR7361,68100 Mulhouse, France
[2] Université de Strasbourg, France
[3] Laboratoire des Couches Minces et Nanomatériaux, Université Abdelmalek Essaâdi, FST, ancienne route de l'aéroport, Km10, Ziaten, BP416, 90050, Tanger, Morocco

E-mail: marie-christine.hanf@uha.fr

Received 3 October 2019, revised 9 December 2019
Accepted for publication 13 January 2020
Published 13 February 2020

Abstract

Silicene and germanene freestanding layers are usually described as a honeycomb lattice formed by two hexagonal sub-lattices presenting a height difference, namely the layer buckling. In this work, first-principles calculations show that silicene and germanene can be rippled at 0 K with various wavelengths, without any compressive strain of the layer. For germanene, the height difference between two Ge atoms from the same sub-lattice can be as high as 4.7 Å for an undulation length of 81 Å. The deformations are related to slight (lower than 1.7°) bond angle modifications, and the energy cost is remarkably low, lying between 0.1 and 0.8 meV per atom. These undulations modify the electronic structure, opening a gap of 15 meV.

Keywords: germanene, undulations, DFT, rippling

(Some figures may appear in colour only in the online journal)

1. Introduction

Since the first experimental descriptions of silicene [1] and germanene [2, 3], these two-dimensionnal (2D) crystals are widely explored, in particular because of their numerous expected applications [4–10], for example in nanoelectronics, in relation with their high carrier mobility [11–13]. Moreover, they could be used as a spin filter [14], gas separation [15], DNA sequencers [16] or for energy conversion and storage applications [17]. They can also be functionalized with organic molecules to modify their properties [17, 18]. They have been mainly grown on metallic substrates, namely on the Ag(1 1 1) surface for silicene [1, 19–21], and Au(1 1 1) [2, 22], Ag(1 1 1) [23] or Al(1 1 1) [3, 24–28] for germanene. However, even if the atoms are arranged in a honeycomb structure, the atomic structure of silicene and germanene is quite different from that expected for a freestanding layer, which is constituted by two equivalent hexagonal sub-lattices, differing by a height difference [29]. In the case of germanene deposited on Ag(1 1 1), two different phases are described, i.e. one which is in part commensurate to the substrate, and a second one close to freestanding germanene [23]. For silicene on Ag(1 1 1) and germanene on Au(1 1 1) or Al(1 1 1), the Si and Ge lattice tends to match that of the substrate, which means that strong interactions between the 2D crystal and the sub-lying surface are present [1, 19, 30–33]. Since the intrinsic electronic properties of germanene and silicene are drastically affected by these interactions [12, 22, 34, 35], different strategies have been proposed to obtain these systems onto other substrates, for which only van der Waals interactions are present. According to density functional theory (DFT) calculations, the 2D layer could be detached, and then deposited on a chosen substrate [36, 37]. On the other hand, germanene has been synthesized by evaporation of Ge, in ultrahigh vacuum, on graphite [38] or MoS_2 [39], and silicene has been obtained on graphite by evaporating Si [40]. The atomic structure of the resulting 2D lattice is close to that of a freestanding layer, and adsorption energy (E_{ads}) calculations indicate a reduction of the interaction strength with respect to metallic substrates. For silicene on graphene, $E_{ads} = 0.08$ eV per Si atom [41], while on silver the energy lies between 0.46 and 0.49 eV [1, 30, 42, 43]. However, the

[4] Author to whom any correspondence should be addressed.

growth of silicene or germanene on these substrates is not easy to carry on [44, 45].

Now, it appears that graphene, the prototypical 2D material, can exhibit out-of-plane deformations, whenever it is suspended or deposited on a substrate [46–50]. In particular, calculations show that graphene naturally wrinkles because of thermal fluctuations [51, 52]. Thus the deposition of germanene and silicene interacting only weakly with the substrate could be made still more difficult if ripples are easily formed. According to molecular dynamics simulations, silicene actually wrinkles, with deformation heights of 3.5 Å at 150 K and 5.4 Å at 300 K [53]. But undulations are not only related to a thermal effect. Indeed calculations indicate that graphene [54], as well as silicene [55], present corrugations at 0 K when applying a compressive strain. However the nature of silicene and germanene is quite different from that of graphene. The latter constitutes the ideal 2D system with sp^2 bonds, while silicene and germanene are buckled and present an sp^2–sp^3 hybridization, with bond angles of 116° (Si) and 112° (Ge), that is, between 109° (pure sp^3) and 120° (pure sp^2). Since in graphene rippling is related to bond angle modifications [54], the sp^2–sp^3 hybridization for silicene and germanene, which results in weaker π-bonds [56], may afford an extra degree of freedom with respect to graphene. In other words, silicene and germanene could present undulations without the need of a compressive strain or thermal effect. Indeed, for graphene, rippling (at 0 K) without applied strain means upward displacements of C atoms, thus an increase of the C–C bonds length, while for silicene or germanene a simple angle modification would be sufficient. In this respect it has been shown that the energy cost to move vertically a C atom is much higher than a Si atom [56], and that the Young modulus of graphene (340 $N \cdot m^{-1}$) is larger than that of silicene (63.8 $N \cdot m^{-1}$) [57].

In this paper, by means of DFT, we describe silicene and germanene freestanding layers presenting different wrinkles heights. The calculation cell size is kept constant, i.e. no compressive strain is applied. We show that the rippled layers are stable at 0 K, and that their deformation energy with respect to the flat layer is lower than 1 meV per atom. However, the electronic band structure is clearly affected by the undulation.

2. Calculations methods

The calculations have been performed thanks to the VASP (Vienna *Ab initio* simulation package) code [58–61], in the generalized gradient approximation, using projector-augmented waves [62, 63] and the functional of Perdew, Burke and Ernzerhof [64, 65]. The different parameters have been thoroughly chosen to ensure that the undulations obtained after relaxation were independent of the calculation conditions. In particular, various maximum values for the forces components have been tested, namely 0.01 $eV\mathring{A}^{-1}$, 0.005 $eV\mathring{A}^{-1}$ and 0.003 $eV\mathring{A}^{-1}$. It appeared that convergence is reached at 0.005 $eV\mathring{A}^{-1}$, which the value used throughout this work. For silicene, a diamond cell of 128 atoms has first been used, with a size of 30.94 Å × 30.94 Å. Undulations along the zig-zag atomic chains of the honeycomb lattice have been studied using rectangular meshes constituted of 32, 48, 64 or 80 atoms, with a size of 30.94 Å × 6.70 Å, 46.41 Å × 6.70 Å, 61.88 Å × 6.70 Å, and 77.35 Å × 6.70 Å respectively. For undulations along the armchair atomic chains, the sizes are 7.74 Å × 26.80 Å, 7.74 Å × 40.19 Å, 7.74 Å × 53.59 Å, and 7.74 Å × 66.99 Å. For germanene, we restricted our study to the meshes of 64 and 80 atoms, which present the largest deformations. The meshes sizes are 64.97 Å × 7.03 Å or 81.21 Å × 7.03 Å for the undulations along the zig-zag direction, and 8.12 Å × 56.27 Å or 8.12 Å × 70.33 Å for the armchair direction. For all systems the cell height was 20 Å. The Brillouin zone of the diamond mesh has been sampled with (3 × 3 × 1) k-points. For the rectangular meshes oriented along the zig-zag direction, (1 × 5 × 3), (2 × 10 × 6) and (3 × 15 × 9) k-points have been tested. We found that convergence is reached for (2 × 10 × 6) k-points, which is the sampling we used. For the rectangular meshes oriented along the armchair direction, (10 × 2 × 6) k-points have been taken. Band structure calculations have been performed with a cut-off energy of 400 eV for silicene, and 450 eV for germanene. Since the used meshes are larger than the 2D layer primitive cell which contains only two atoms, the bands have been unfolded using the bandUP code [66].

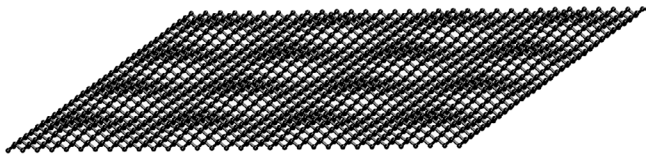

Figure 1. Relaxed silicene layer with undulations in two directions.

The calculated lattice parameters for germanene (4.061 Å) and silicene (3.868 Å) result from the optimization of the flat layers, using a mesh containing two Ge or Si atoms and (31 × 31 × 11) k-points. Note that in this paper we define as 'flat' germanene or silicene the usual low-buckled ($\Delta h = 0.688$ Å for germanene and 0.449 Å for silicene) honeycomb lattice, for which no ripples are present. The obtained parameter and buckling values are in agreement with previous works [29, 67, 68]. The atomic structures are presented using the visual dynamic software developed by the Theoretical and Computational Biophysics Group in the Beckman Institute for Advanced Science and Technology at the University of Illinois at Urbana Champaign [69, 70].

3. Results and discussion

3.1. Structural study

First we deformed a diamond silicene mesh (128 atoms, mesh size: 30.94 Å) by displacing the Si atoms vertically at different heights. Figure 1 presents several repeated unit cells after relaxation. The system does not appear as a freestanding flat layer, but presents undulations in two directions, namely along armchair and zigzag chains, with a maximum height difference of 0.45 Å between two atoms from the same sublattice. In order to have quantitative results, and to perform

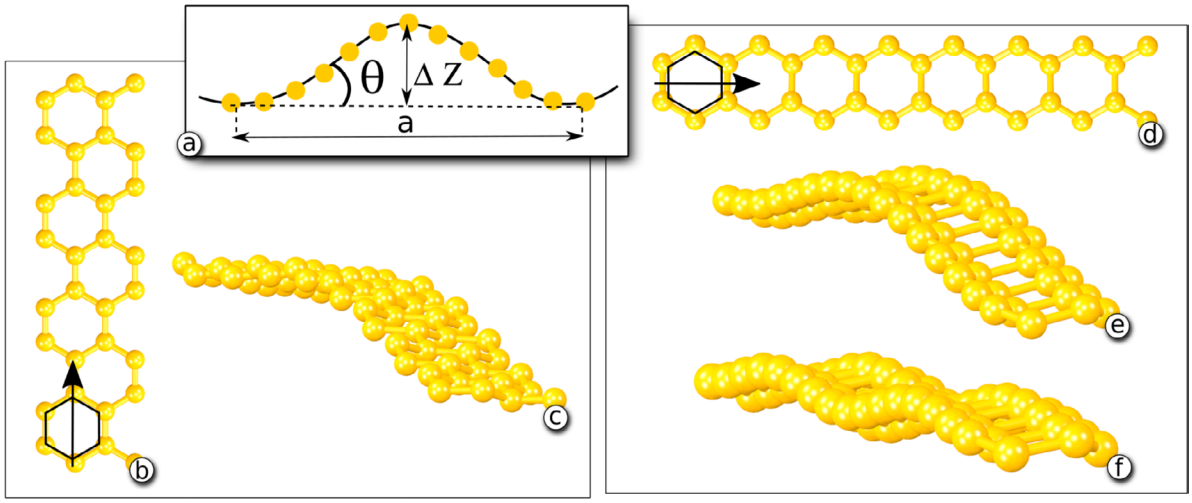

Figure 2. (a) Description of the height difference Δz, the gradient angle θ, and the mesh length a. Ball-and-stick silicene models presenting one single mesh after relaxation with undulations along the armchair direction: (b) top view, mesh of 32 atoms; (c) side-view, mesh of 64 atoms. Undulations along the zig-zag direction: (d) top view, mesh of 32 atoms; (e) side-view, mesh of 64 atoms; (f) side-view, two undulations for a mesh of 64 atoms. The arrows indicate the undulation direction.

calculations on larger systems, we studied 2D layers that are rippled along one single direction, either parallel to the zigzag or to the armchair chains. The rectangular meshes are first deformed by placing all the atoms of a given zigzag or armchair chain at different heights in order to obtain a wave, so that all the atoms (for one of the two sub-lattices) of a chain perpendicular to the undulation direction are at the same height. The mesh size is the same for the flat and the deformed layer. The systems are then relaxed for various initial undulation heights. Figure 2, which displays different meshes after relaxation, shows that the layer is still rippled. We also tested a mesh presenting initially two undulations, which subsist after relaxation (figure 2(f)).

For the different mesh sizes, we find that for a low initial deformation, the system is almost not modified after relaxation. In contrast, when the initial height difference is rather high, the layer tends to minimize the inter-atomic forces, and to reduce the undulation height. In fact, each mesh size can be related to one maximum value for Δz, where Δz is the height difference between the highest and the lowest atom for a given sub-lattice (see figure 2(a)). One can see, in figure 3(a), that $\Delta z_{\max}$, i.e. the highest value for Δz, increases with the mesh length, and ranges between 0.67 Å and 4.65 Å. It appears that the unidirectional ripples can be fitted by means of a cosine function. More precisely, the positions of the atoms belonging to the highest sub-lattice are given by $z(x) = z_{\max}\cos(Kx)$. For example, for undulations oriented along the zig-zag direction, the values for the 80 atoms silicene (germanene) mesh are $z_{\max} = 2.04$ Å (2.25 Å) and $K = 0.0812$ Å^{-1} (0.0774 Å^{-1}).

Now the question is to know whether the augmentation of the maximal height variation is only related to the increasing mesh length. Thus we calculated the gradient angle θ in the following way: $\tan\theta = \frac{\Delta z_{\max}}{0.5a}$, where a is the mesh length. According to figure 3(b), the gradient angle θ lies between 2.8° and 6.7°, and, for a given mesh size, is larger for germanene

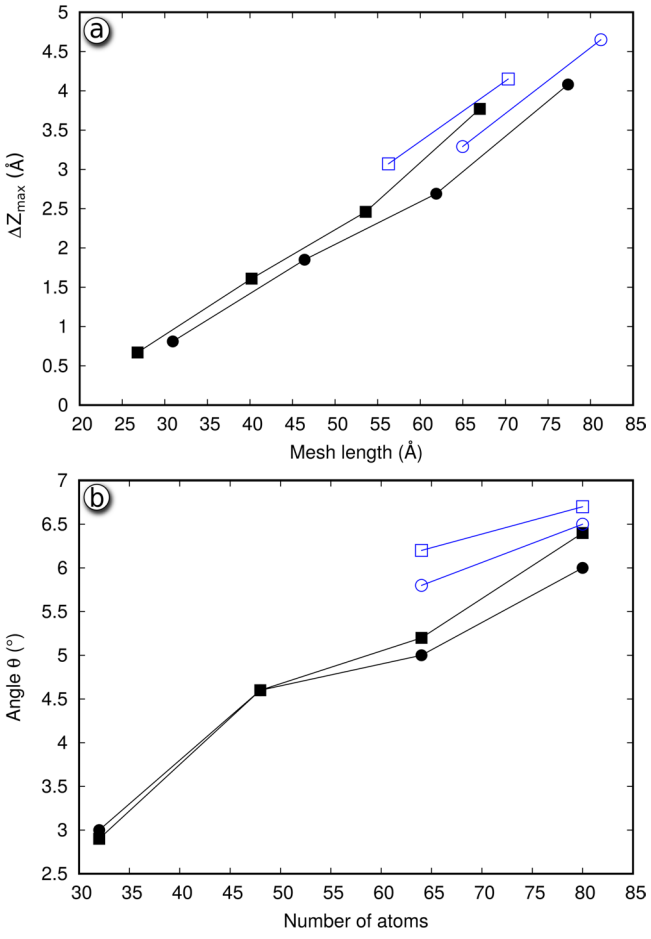

Figure 3. (a) Maximum height difference Δz (in Å) as a function of the mesh length (in Å); (b) gradient angle θ (in °) as a function of the number N of atoms in the mesh. The solid (empty) symbols correspond to silicene (germanene). For germanene, only the largest meshes are presented in order to obtain the trends. The squares (circles) refer to undulations oriented along the armchair (zig-zag) direction.

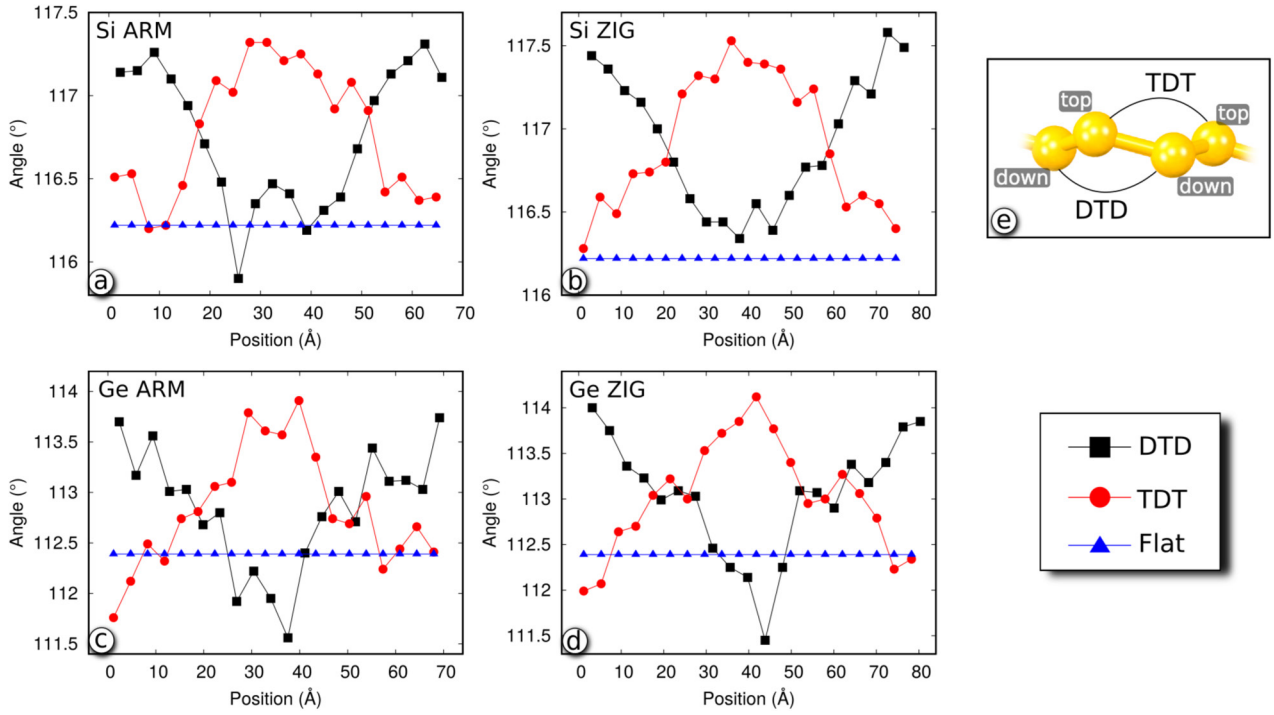

Figure 4. Bond angles (in °) as a function of the atom position (in Å) within the atomic chain, for meshes containing 80 atoms. The circles (squares) correspond to TDT (DTD) bonds, and the triangles to the flat freestanding layer. (a) Silicene, armchair direction; (b) silicene, zig-zag direction; (c) germanene, armchair direction; (d) germanene, zig-zag direction; (e) sketch presenting the TDT and DTD angles.

Table 1. Energy per atom and deformation energy, in eV, for silicene and germanene as a function of the atoms number N in the mesh, for one undulation per mesh along the armchair or zigzag direction.

		Silicene				Germanene	
	N (atoms number)	32	48	64	80	64	80
Armchair	Atom energy	−4.7848	−4.7848	−4.7848	−4.7842	−4.0126	−4.0124
	Deformation energy	0.0002	0.0002	0.0002	0.0008	0.0007	0.0009
Zigzag	Atom energy	−4.7849	−4.7846	−4.7846	−4.7843	−4.0125	−4.0125
	Deformation energy	0.0001	0.0004	0.0004	0.0007	0.0008	0.0008

than for silicene. Moreover, it increases with the number of atoms N within the mesh. In other words, the maximum height variation is not just proportional to the undulation length, since in that case θ would be similar for the different values of N. Thus we are looking for what induces the augmentation of the gradient angle.

Our calculations show that the layer deformation is not related to a bond extension, since the Si–Si (Ge–Ge) length lies between 2.28 Å and 2.29 Å (2.45 Å and 2.46 Å), while for the flat layer the value is 2.28 Å (2.44 Å). As a result, the ripples must result from a variation of the bond angles with respect to that of the flat layers, namely 116.22° for silicene, and 112.41° for germanene. It appears that the mean bond angle actually increases, but only slightly, from 0.1° to 0.7°. Therefore it is useful to have a picture of the local angles variations, as displayed in figure 4, which gives the bond angle value for every Si or Ge atom along an armchair or zigzag chain in one mesh. Two types of bonds have to be distinguished, as indicated in figure 4(e), namely down-top-down (DTD) bonds or top-down-top bonds (TDT). Note that for a flat layer the DTD and TDT bonds are the same since the sub-lattices of the top and down atoms are equivalent.

The difference between the largest and smallest bond angle is about 1.2° for silicene and 2.3° for germanene. The atom for which the DTD bond angle is maximum is the nearest neighbor of the one exhibiting the lowest TDT bond, and vice versa. Moreover the largest deformations with respect to the flat layer are located at the convex parts of the layer. We should note that, according to the calculations of Peng *et al*, the Young modulus of buckled silicene (63.8 $N \cdot m^{-1}$) is lower than that of flat silicene (71.2 $N \cdot m^{-1}$) [57], which indicates the additional degree of freedom of sp^2–sp^3 bonds with respect to pure sp^2 ones. It appears that the Ge bonds are more easily deformed than the Si ones, which is also reflected in a Young modulus of 44 $N \cdot m^{-1}$ [71], that is, lower than for buckled silicene. Finally, we calculated the average effective bond angles (AEBA) which allows to indicate the sp^3 (AEBA1) or sp^2 (AEBA2) character of a bond hybridization [72]. The AEBA is obtained as following:

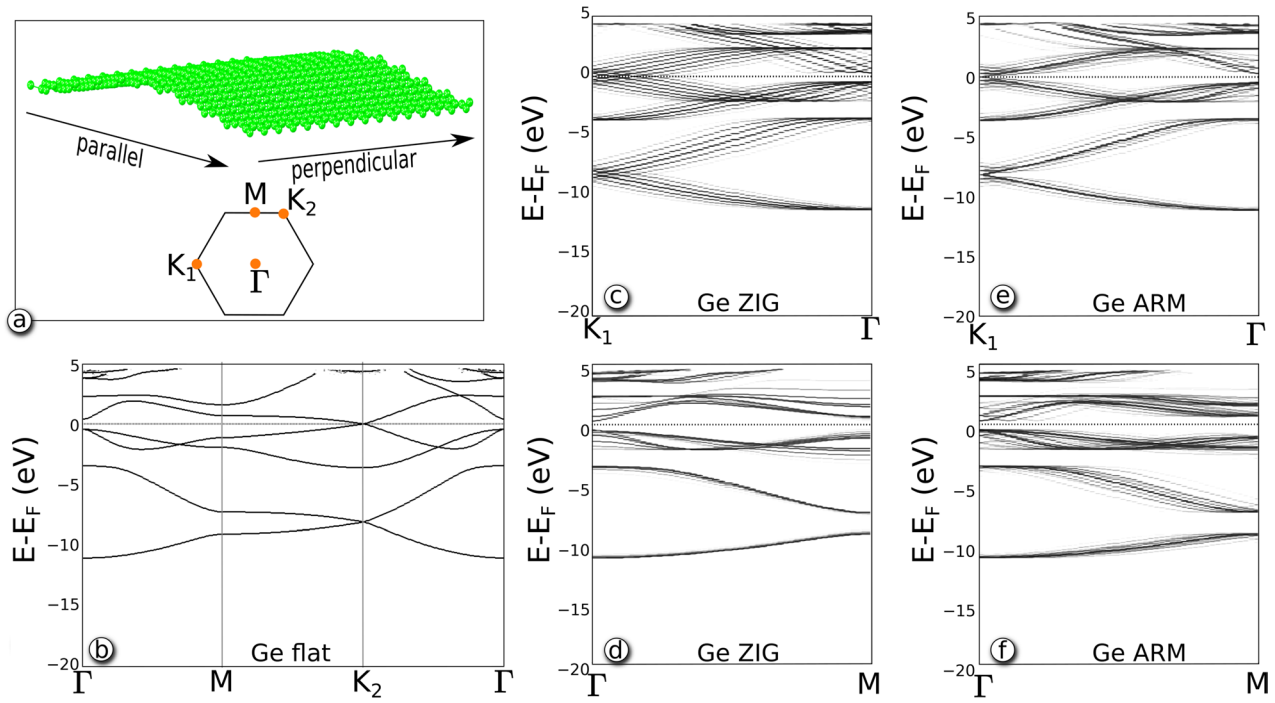

Figure 5. Band structure of germanene for a mesh comprising 80 atoms for (b) a flat layer, (c) undulations oriented along the zig-zag direction, the $K_1\Gamma$ direction (indicated in (a)) is parallel to the undulation; (d) undulations oriented along the zig-zag direction, the ΓM direction is perpendicular to the undulation; (e) undulations oriented along the armchair direction, the $K_1\Gamma$ direction is perpendicular to the undulation (f) undulations oriented along the armchair direction, the ΓM direction is parallel to the undulation. For the flat layer, the K_1 and K_2 points are equivalent.

$$\mathrm{AEBA} = 1 - \frac{\sum_{i=1}^{N_{\mathrm{angle}}} |A - \mathrm{Ang}(i)|}{A \cdot N_{\mathrm{angle}}} \qquad (1)$$

with $A = 109.47°$ for AEBA1, and $A = 120°$ for AEBA2. [72]. For flat silicene, AEBA1 $= 0.938$ while AEBA2 $= 0.968$, indicating that the hybridization is more sp^2 than sp^3, as mentioned in the work of Guo *et al*. For a silicene mesh containing 80 atoms, AEBA1 $= 0.932$ and AEBA2 $= 0.974$ (zig-zag direction), or AEBA1 $= 0.933$ and AEBA2 $= 0.973$ (armchair direction). We can see that rippling induces a slight diminution of the sp^3 character, and thus an increase of the sp^2 nature of the bond. With regard to germanene, we obtain AEBA1 $= 0.973$, 0.967, and 0.969 for the flat layer, the system undulated along the zig-zag direction, and along the armchair direction, respectively. The values for AEBA2 are 0.937, 0.942, and 0.940. Thus, for germanene, the hybridization is more sp^3 than sp^2 for both the flat and wrinkled layers. However, as for silicene, there is an augmentation of the sp^2 nature of the hybridization upon rippling. The influence of this wrinkling on the silicene and germanene total energy is the subject of the following section.

3.2. Energetic study

In table 1, we compare the energy per atom for various mesh sizes to that corresponding to the flat layer, namely -4.7850 eV and -4.0133 eV for silicene and germanene, respectively. The data are taken for the systems presented in figure 3, which exhibit the largest height difference Δz_{max}.

Clearly the energy difference between the wrinkled and the flat layers, which ranges between 0.1 and 0.8 meV per atom, is very low, which is in line with the very small bond angles deformations. Thus the different configurations can be considered as energetically equivalent. Moreover, for height differences lower than Δz_{max} (for a given mesh size a), the deformation energies are smaller than those given in table 1. In other words, an infinity of energy-degenerated configurations can be found, with various undulation lengths a, and with various height deformations Δz, varying continuously from $\Delta z = 0$ to $\Delta z = \Delta z_{\mathrm{max}}$ (a). There is no energy barrier between two different configurations, and one given configuration is not more or less stable than another. We must emphasize that for graphene the energy cost due to ripples formation at 0 K, with a gradient angle smaller than 10°, lies below 1 meV per C atom [73]. However one has to keep in mind that, contrary to silicene and germanene, undulations in graphene result from a compressive strain.

3.3. Electronic study

In freestanding silicene or germanene, the atomic environment is the same for all atoms. This is not the case in a rippled layer, since the bond angles differ from one atom to another, as shown in figure 4. Thus the electronic structure is expected to change upon wrinkling. We performed band structure calculations for the germanene mesh of 80 atoms, which is the system displaying the largest angular modifications. The results are presented in figure 5, for both the flat and

undulated layer. The points in the Brillouin zone have been chosen in the following way: when the germanene is rippled along the zigzag atomic chains, the $K_1\Gamma$ (ΓM) direction is parallel (perpendicular) to the undulation (see figure 5(a) and top-views in figure 2) . In contrast, when the germanene is rippled along the armchair atomic chains, the $K_1\Gamma$ (ΓM) direction is perpendicular (parallel) to the undulation.

It appears that, for the undulated layer, the bands characterizing the flat layer are still visible. However they are split because the atomic sites are not equivalent when the system is wrinkled. Moreover our calculations show that there is a gap opening at the K_1 point of about 15 meV for both undulations directions. We would like to emphasize that for corrugated graphene, the maximum gap value is 5 meV for a gradient angle of 10° [73]. Here the gradient angle is lower than 7° (see figure 3), for a gap of about 15 meV. Thus rippling has a larger effect for gemanene than for graphene. Moreover, according to figure 4, the Ge–Ge–Ge bond angle varies from −0.7° to 1.5° with respect to flat germanene. Now, Wang *et al* have shown that a gap of 13.7 meV appears, when toluene is physisorbed on freestanding germanene, while the bond angle modifications with respect to pristine germanene lie between −1.4 and 0.7° [74]. Thus the gap opening may be related to bond angle modifications. However, in this latter case the germanene deformation is induced by the presence of physical interactions with the molecule, whereas for undulated germanene, the gap opening results from an internal modification of the system.

Finally, one can see in figure 5 that the band structure depends on the orientation of the undulation. When the bands are analyzed along a direction which is parallel to the undulation (figures 5(c) and (f)) the bands resulting from the splitting exhibit a larger weight and a larger energy extension than in the case of a direction perpendicular to the undulation (figures 5(d) and (e)). Indeed, in figures 5(c) and (f), the atoms of a given atomic chain are positioned in various heights since the undulation is parallel to the chain. In contrast, when the $K_1\Gamma$ or ΓM directions are perpendicular to the undulation, the atomic z positions for a chain are similar, while the height of the different chains varies along the mesh. This anisotropy in the atomic positions results in an anisotropy in the electronic structure.

4. Conclusion

2D materials such as silicene and germanene can be rippled without noticeable total energy difference with respect to the flat layers. The undulations are not related to an augmentation of the bond length, but to slight modifications of the bond angles. The addition of the different bond angles deformations induces an increase of the undulation height with the undulation length. As a result, the atoms present various atomic environments, which induce a splitting in the band structure and a gap opening of about 15 meV. This rippling effect is quite different from what is observed for graphene. Since the latter is characterized by sp^2 C–C bonds, undulations at 0 K are obtained only after a compression of the system. In contrast, silicene and germanene may wrinkle without applied strain because of the softness of the sp^2–sp^3 bond angles. This property can probably be extended to other low-buckled 2D systems formed from column IV elements, such as stanene [75, 76], or plumbene [77, 78].

Finally, the usual picture of silicene or germanene as a flat layer is largely incomplete. This is only one conformation among many other ones, for which the systems present undulations at 0 K with various heights and lengths, but with similar total energy. It can be expected that the thermal energy brought by $T > 0$ will facilitate the formation of ripples in the layer, which must be taken into account if silicene or germanene are to be detached from their growing substrate and deposited on another support.

Acknowledgments

The authors would like to acknowledge the High Performance Computing center of the University of Strasbourg for supporting this work by providing scientific support and access to computing resources. Part of the computing resources was funded by the Equipex Equip@Meso project Programme Investissements d'Avenir and the CPER Alsacalcul/Big Data.

The calculations have also been performed with a financial support from Campus France (Toubkal No 34721YK), and the French National Research Agency (ANR-17-CE09-0021-03).

ORCID iDs

M-C Hanf https://orcid.org/0000-0003-1820-504X
M Zanouni https://orcid.org/0000-0002-8446-6259
Ph Sonnet https://orcid.org/0000-0001-5891-5500

References

[1] Vogt P, De Padova P, Quaresima C, Avila J, Frantzeskakis E, Asensio M C, Resta A, Ealet B and Le Lay G 2012 Silicene: compelling experimental evidence for graphenelike two-dimensional silicon *Phys. Rev. Lett.* **108** 155501

[2] Dávila M E, Xian L, Cahangirov S, Rubio A and Lay G L 2014 Germanene: a novel two-dimensional germanium allotrope akin to graphene and silicene *New J. Phys.* **16** 095002

[3] Derivaz M, Dentel D, Stephan R, Hanf M-C, Mehdaoui A, Sonnet P and Pirri C 2015 Continuous germanene layer on Al(1 1 1) *Nano Lett.* **15** 2510–6

[4] Acun A *et al* 2015 Germanene: the germanium analogue of graphene *J. Phys.: Condens. Matter* **27** 443002

[5] Li G, Zhang Y-Y, Guo H, Huang L, Lu H, Lin X, Wang Y-L, Du S and Gao H-J 2018 Epitaxial growth and physical properties of 2D materials beyond graphene: from monatomic materials to binary compounds *Chem. Soc. Rev.* **47** 6073–100

[6] Balendhran S, Walia S, Nili H, Sriram S and Bhaskaran M 2015 Elemental analogues of graphene: silicene, germanene, stanene, and phosphorene *Small* **11** 640–52

[7] Ezawa M, Salomon E, De Padova P, Solonenko D, Vogt P, Dávila M, Molle A, Angot T and Le Lay G 2018

Fundamentals and functionalities of silicene, germanene, and stanene *Riv. Nuovo Cimento* **41** 175–224
[8] Patel K, Roondhe B, Dabhi S D and Jha P K 2018 A new flatland buddy as toxic gas scavenger: a first principles study *J. Hazardous Mater.* **351** 337–45
[9] Patel P D, Shinde S, Gupta S D and Jha P K 2019 Investigation of structural and elastic stability, electronic, magnetic, thermoelectric, lattice-dynamical and thermodynamical properties of spin gapless semiconducting heusler alloy Zr_2MnIn using DFT approach *J. Electron. Mater.* **48** 1634–42
[10] Roondhe B and Jha P K 2018 'Haeckelite', a new low dimensional cousin of boron nitride for biosensing with ultra-fast recovery time: a first principles investigation *J. Mater. Chem.* B **6** 6796–807
[11] Molle A, Grazianetti C, Tao L, Taneja D, Alam M H and Akinwande D 2018 Silicene, silicene derivatives, and their device applications *Chem. Soc. Rev.* **47** 6370–87
[12] Takagi N, Lin C-L, Kawahara K, Minamitani E, Tsukahara N, Kawai M and Arafune R 2015 Silicene on Ag(1 1 1): geometric and electronic structures of a new honeycomb material of Si *Prog. Surf. Sci.* **90** 1–20
[13] Tao L, Cinquanta E, Chiappe D, Grazianetti C, Fanciulli M, Dubey M, Molle A and Akinwande D 2015 Silicene field-effect transistors operating at room temperature *Nat. Nanotechnol.* **10** 227
[14] Rachel S and Ezawa M 2014 Giant magnetoresistance and perfect spin filter in silicene, germanene, and stanene *Phys. Rev.* B **89** 195303
[15] Hu W, Wu X, Li Z and Yang J 2013 Porous silicene as a hydrogen purification membrane *Phys. Chem. Chem. Phys.* **15** 5753–7
[16] Sadeghi H, Bailey S and Lambert C J 2014 Silicene-based DNA nucleobase sensing *Appl. Phys. Lett.* **104** 103104
[17] Liu N, Bo G, Liu Y, Xu X, Du Y and Dou S X 2019 Recent progress on germanene and functionalized germanene: preparation, characterizations, applications, and challenges *Small* **15** 1805147
[18] Brennan M D, Morishita T and Spencer M J S 2016 Tuning the band gap of silicene by functionalisation with naphthyl and anthracyl groups *J. Chem. Phys.* **144** 114704
[19] Johnson N W, Vogt P, Resta A, De Padova P, Perez I, Muir D, Kurmaev E Z, Le Lay G and Moewes A 2014 The metallic nature of epitaxial silicene monolayers on Ag(1 1 1) *Adv. Funct. Mater.* **24** 5253–9
[20] Liu Z-L, Wang M-X, Xu J-P, Ge J-F, Lay G L, Vogt P, Qian D, Gao C-L, Liu C and Jia J-F 2014 Various atomic structures of monolayer silicene fabricated on Ag(1 1 1) *New J. Phys.* **16** 075006
[21] Bernard R, Borensztein Y, Cruguel H, Lazzeri M and Prévot G 2015 Growth mechanism of silicene on Ag(1 1 1) determined by scanning tunneling microscopy measurements and *ab initio* calculations *Phys. Rev.* B **92** 045415
[22] Dávila M E and Lay G L 2016 Few layer epitaxial germanene: a novel two-dimensional Dirac material *Sci. Rep.* **6** 20714
[23] Lin C-H *et al* 2018 Single-layer dual germanene phases on Ag(1 1 1) *Phys. Rev. Mater.* **2** 024003
[24] Stephan R, Hanf M, Derivaz M, Dentel D, Asensio M C, Avila J, Mehdaoui A, Sonnet P and Pirri C 2016 Germanene on Al(1 1 1): interface electronic states and charge transfer *J. Phys. Chem.* C **120** 1580–5
[25] Endo S, Kubo O, Nakashima N, Iwaguma S, Yamamoto R, Kamakura Y, Tabata H and Katayama M 2017 $\sqrt{3} \times \sqrt{3}$ germanene on Al(1 1 1) grown at nearly room temperature *Appl. Phys. Express* **11** 015502
[26] Wang W and Uhrberg R I G 2017 Coexistence of strongly buckled germanene phases on Al(1 1 1) *Beilstein J. Nanotechnol.* **8** 1946–51
[27] Fukaya Y, Matsuda I, Feng B, Mochizuki I, Hyodo T and Shamoto S-I 2016 Asymmetric structure of germanene on an Al(1 1 1) surface studied by total-reflection high-energy positron diffraction *2D Mater.* **3** 035019
[28] Martínez E A, Fuhr J D, Grizzi O, Sánchez E A and Cantero E D 2019 Growth of germanene on Al(1 1 1) hindered by surface alloy formation *J. Phys. Chem.* C **123** 12910–8
[29] Cahangirov S, Topsakal M, Aktürk E, Şahin H and Ciraci S 2009 Two- and one-dimensional honeycomb structures of silicon and germanium *Phys. Rev. Lett.* **102** 236804
[30] Stephan R, Hanf M-C and Sonnet P 2015 Spatial analysis of interactions at the silicene/Ag interface: first principles study *J. Phys.: Condens. Matter* **27** 015002
[31] Wang W and Uhrberg R I G 2017 Investigation of the atomic and electronic structures of highly ordered two-dimensional germanium on Au(1 1 1) *Phys. Rev. Mater.* **1** 074002
[32] Stephan R, Derivaz M, Hanf M-C, Dentel D, Massara N, Mehdaoui A, Sonnet P and Pirri C 2017 Tip-induced switch of germanene atomic structure *J. Phys. Chem. Lett.* **8** 4587–93
[33] Marjaoui A, Stephan R, Hanf M-C, Diani M and Sonnet P 2016 Tailoring the germanene substrate interactions by means of hydrogenation *Phys. Chem. Chem. Phys.* **18** 15667–72
[34] Mahatha S K, Moras P, Bellini V, Sheverdyaeva P M, Struzzi C, Petaccia L and Carbone C 2014 Silicene on Ag(1 1 1): a honeycomb lattice without Dirac bands *Phys. Rev.* B **89** 201416
[35] Cahangirov S, Audiffred M, Tang P, Iacomino A, Duan W, Merino G and Rubio A 2013 Electronic structure of silicene on Ag(1 1 1): strong hybridization effects *Phys. Rev.* B **88** 035432
[36] Tsetseris L and Kaltsas D 2014 Chemical routes to modify, uplift, and detach a silicene layer from a metal substrate *Phys. Chem. Chem. Phys.* **16** 5183–7
[37] Kaloni T P and Schwingenschlgl U 2013 Weak interaction between germanene and GaAs(0 0 0 1) by H intercalation: a route to exfoliation *J. Appl. Phys.* **114** 184307
[38] Persichetti L, Jardali F, Vach H, Sgarlata A, Berbezier I, De Crescenzi M and Balzarotti A 2016 van der Waals heteroepitaxy of germanene islands on graphite *J. Phys. Chem. Lett.* **7** 3246–51
[39] Zhang L, Bampoulis P, Rudenko A N, Yao Q, van Houselt A, Poelsema B, Katsnelson M I and Zandvliet H J W 2016 Structural and electronic properties of germanene on MoS_2 *Phys. Rev. Lett.* **116** 256804
[40] De Crescenzi M, Berbezier I, Scarselli M, Castrucci P, Abbarchi M, Ronda A, Jardali F, Park J and Vach H 2016 Formation of silicene nanosheets on graphite *ACS Nano* **10** 11163–71
[41] Cai Y, Chuu C-P, Wei C M and Chou M Y 2013 Stability and electronic properties of two-dimensional silicene and germanene on graphene *Phys. Rev.* B **88** 245408
[42] Enriquez H, Vizzini S, Kara A, Lalmi B and Oughaddou H 2012 Silicene structures on silver surfaces *J. Phys.: Condens. Matter* **24** 314211
[43] Tchalala M R, Enriquez H, Yildirim H, Kara A, Mayne A J, Dujardin G, Ali M A and Oughaddou H 2014 Atomic and electronic structures of the $\sqrt{13} \times \sqrt{13}$R13.9° of silicene sheet on Ag(1 1 1) *Appl. Surf. Sci.* **303** 61–6
[44] Peng W *et al* 2018 Resolving the controversial existence of silicene and germanene nanosheets grown on graphite *ACS Nano* **12** 4754–60
[45] van Bremen R, Yao Q, Banerjee S, Cakir D, Oncel N and Zandvliet H 2017 Intercalation of Si between MoS_2 layers *Beilstein J. Nanotechnol.* **8** 1952–60
[46] Meyer J C, Geim A K, Katsnelson M I, Novoselov K S, Booth T J and Roth S 2009 The structure of suspended graphene sheets *Nature* **446** 60

[47] Nicholl R J T, Lavrik N V, Vlassiouk I, Srijanto B R and Bolotin K I 2017 Hidden area and mechanical nonlinearities in freestanding graphene *Phys. Rev. Lett.* **118** 266101
[48] Shen X, Lin X, Yousefi N, Jia J and Kim J-K 2014 Wrinkling in graphene sheets and graphene oxide papers *Carbon* **66** 84–92
[49] Wei Y and Yang R 2018 Nanomechanics of graphene *Natl Sci. Rev.* **6** 324–48
[50] Bangert U, Gass M H, Bleloch A L, Nair R R and Geim A K 2009 Manifestation of ripples in free-standing graphene in lattice images obtained in an aberration-corrected scanning transmission electron microscope *Phys. Status Solidi* a **206** 1117–22
[51] Fasolino A, Los J H and Katsnelson M I 2007 Intrinsic ripples in graphene *Nat. Mater.* **6** 858
[52] Wang W, Li S, Min J and Shen C 2015 Relaxation properties of single layer graphene on SiO_2 substrate *J. Nanosci. Nanotechnol.* **15** 2970–5
[53] Cherukara M J, Narayanan B, Kinaci A, Sasikumar K, Gray S K, Chan M K and Sankaranarayanan S K R S 2016 *Ab initio*-based bond order potential to investigate low thermal conductivity of stanene nanostructures *J. Phys. Chem. Lett.* **7** 3752
[54] Zhang Y and Liu F 2011 Maximum asymmetry in strain induced mechanical instability of graphene: compression versus tension *Appl. Phys. Lett.* **99** 241908
[55] Podsiadły-Paszkowska A and Krawiec M 2016 Electrical and mechanical controlling of the kinetic and magnetic properties of hydrogen atoms on free-standing silicene *J. Phys.: Condens. Matter* **28** 284004
[56] Pizzochero M, Bonfanti M and Martinazzo R 2016 Hydrogen on silicene: like or unlike graphene? *Phys. Chem. Chem. Phys.* **18** 15654–66
[57] Peng Q, Wen X and De S 2013 Mechanical stabilities of silicene *RSC Adv.* **3** 13772–81
[58] Kresse G and Hafner J 1993 *Ab initio* molecular dynamics for liquid metals *Phys. Rev.* B **47** 558
[59] Kresse G and Hafner J 1994 *Ab initio* molecular-dynamics simulation of the liquid-metal–amorphous-semiconductor transition in germanium *Phys. Rev.* B **49** 14251
[60] Kresse G and Furthmüller J 1996 Efficiency of *ab initio* total energy calculations for metals and semiconductors using a plane-wave basis set *Comput. Mater. Sci.* **6** 15–50
[61] Kresse G and Furthmüller J 1996 Efficient iterative schemes for *ab initio* total-energy calculations using a plane-wave basis set *Phys. Rev.* B **54** 11169
[62] Blöchl P E 1994 Projector augmented-wave method *Phys. Rev.* B **50** 17953
[63] Kresse G and Joubert D 1999 From ultrasoft pseudopotentials to the projector augmented-wave method *Phys. Rev.* B **59** 1758
[64] Perdew J P, Burke K and Ernzerhof M 1996 Generalized gradient approximation made simple *Phys. Rev. Lett.* **77** 3865
[65] Perdew J P, Burke K and Ernzerhof M 1997 Generalized gradient approximation made simple *Phys. Rev. Lett.* **78** 1396 (erratum)
[66] Medeiros P V C, Stafström S and Björk J 2014 Effects of extrinsic and intrinsic perturbations on the electronic structure of graphene: retaining an effective primitive cell band structure by band unfolding *Phys. Rev.* B **89** 041407
[67] Li R, Liu Z, Ma W and Tan Y 2016 Strain field of the monovacancy in silicene: first-principles study *AIP Adv.* **6** 055204
[68] Li S-J, Su Y and Chen G 2015 Patterning germanene into superlattices: an efficient method for tuning conducting properties *Chem. Phys. Lett.* **638** 187–90
[69] Humphrey W, Dalke A and Schulten K 1996 VMD: visual molecular dynamics *J. Mol. Graph.* **14** 33–8
[70] Theoretical and Computational Biophysics Group, Visual Molecular Dynamics software, Beckman Institute for Advanced Science and Technology, University of Illinois (www.ks.uiuc.edu/Research/vmd/)
[71] Mortazavi B, Rahaman O, Makaremi M, Dianat A, Cuniberti G and Rabczuk T 2017 First-principles investigation of mechanical properties of silicene, germanene and stanene *Physica* E **87** 228–32
[72] Guo Z-X, Zhang Y-Y, Xiang H, Gong X-G and Oshiyama A 2015 Structural evolution and optoelectronic applications of multilayer silicene *Phys. Rev.* B **92** 201413
[73] Okada S and Kawai T 2012 Electronic structure of corrugated graphene sheet *Japan. J. Appl. Phys.* **51** 02BN05
[74] Wang Y-P, Ji W-X, Zhang C-W, Li S-S, Li F, Li P, Ren M-J, Chen X-L, Yuan M and Wang P-J 2016 Enhanced band gap opening in germanene by organic molecule adsorption *Mater. Chem. Phys.* **173** 379–84
[75] Saxena S, Chaudhary R P and Shukla S 2016 Stanene: atomically thick free-standing layer of 2D hexagonal tin *Sci. Rep.* **6** 31073
[76] Shodja H M, Ojaghnezhad F, Etehadieh A and Tabatabaei M 2017 Elastic moduli tensors, ideal strength, and morphology of stanene based on an enhanced continuum model and first principles *Mech. Mater.* **110** 1–15
[77] Lu D, Zhou Y H, Wang S A, Yang T and Jiang J Z 2016 Topological properties of atomic lead film with honeycomb structure *Sci. Rep.* **6** 21723
[78] Li Y, Zhang J, Zhao B, Xue Y and Yang Z 2019 Constructive coupling effect of topological states and topological phase transitions in plumbene *Phys. Rev.* B **99** 195402